NEOPLASIA
www.neoplasia.com

Volume 10 Number 8 August 2008 pp. 817–827 817

Generation and Characterization of Novel Local and Metastatic Human Neuroblastoma Variants[1,2]

Ido Nevo*, Orit Sagi-Assif*, Liat Edry Botzer*, Dana Amar*, Shelly Maman*, Naam Kariv†, Leonor E. Leider-Trejo‡, Larissa Savelyeva§, Manfred Schwab§, Ilana Yron* and Isaac P. Witz*

*Department of Cell Research and Immunology, George S. Wise Faculty of Life Sciences, Tel-Aviv University, Tel-Aviv, Israel; †Animal Care Facilities, Sackler Faculty of Medicine, Tel-Aviv University, Tel-Aviv, Israel; ‡Institute of Pathology, Tel-Aviv Sourasky Medical Center, Tel-Aviv, Israel; §Department of Tumor Genetics (B030), German Cancer Research Center, Heidelberg, Germany

Abstract

Neuroblastoma (NB) is the most commonly occurring solid tumor in children. The disease usually arises in the adrenal medulla, and it is characterized by a remarkable heterogeneity in its progression. Most NB patients with an advanced disease have massive bone marrow infiltration at diagnosis. Lung metastasis represents a widely disseminated stage and is typically considered to be a terminal event. Much like other malignancies, NB progression is a complex, multistep process. The expression, function, and significance of the various factors involved in NB progression must be studied in relevant *in vivo* and *in vitro* models. Currently, models consisting of metastatic and nonmetastatic cell variants of the same genetic background exist for several types of cancer; however, none exists for NB. In the present study, we describe the generation of a NB metastasis model. SH-SY5Y and MHH-NB-11 NB cells were inoculated orthotopically into the adrenal glands of athymic nude mice. Neuroblastoma cells metastasizing to the lungs were isolated from mice bearing adrenal tumors. Lung metastatic variants were generated by repeated cycles of *in vivo* passage. Characterization of these variants included cellular morphology and immunophenotyping *in vitro*, aggressiveness *in vivo*, and various biologic parameters *in vitro*. The NB metastatic variant in each model displayed unique properties, and both metastatic variants demonstrated a metastatic phenotype *in vivo*. These reproducible models of human NB metastasis will serve as an unlimited source of transcriptomic and proteomic material. Such models can facilitate future studies on NB metastasis and the identification of novel NB biomarkers and targets for therapy.

Neoplasia (2008) 10, 817–827

Introduction

Neuroblastoma (NB) is a sympathetic nervous system malignancy that accounts for approximately 8% of malignancies in patients younger than 15 years. This tumor originates from the embryonic neural crest, and it occurs most commonly in the adrenal gland [1].

Children older than 1 year of age, with a widespread metastatic disease or with a large, aggressive, localized tumor, have a poor long-term survival rate of approximately 30% [2,3]. The NB disseminates either by hematogenous spread, producing metastasis most frequently in bone marrow, bone, liver, and skin, or by lymphatic spread

Address all correspondence to: Isaac P. Witz, Department of Cell Research and Immunology, George S. Wise Faculty of Life Sciences, Tel-Aviv University, Tel-Aviv 69978, Israel. E-mail: ipwitz@post.tau.ac.il

[1]This study was supported by a grant from Bonnie and Steven Stern (New York, NY).
[2]This article refers to a supplementary material, which is designated by Figure W1 and is available online at www.neoplasia.com.
Received 20 March 2008; Revised 18 May 2008; Accepted 19 May 2008

DOI 10.1593/neo.08402

to regional and distant lymph nodes [4,5]. Lung metastases are considered a terminal event representing a widely disseminated metastatic disease [6–8].

Metastasis is a highly selective and sequential process that requires the coordinated action of many genes. This process includes loss of cellular adhesion, increased motility and invasiveness, entry and survival in the circulation, exit into new tissue, and eventual colonization of a distant site [9–11]. The outcome of this process depends on both the intrinsic properties of the tumor cells and the organ microenvironment [11,12].

In vitro and *in vivo* models for NB metastasis are essential for studies dealing with all aspects of this process and for the design of novel cancer therapy modalities [13–17]. A model that comprises metastatic and nonmetastatic cell variants originating from the same primary tumor would facilitate the identification of genes and gene products linked to metastasis. Such variants have a common genetic background but may differ in the metastasis-associated genetic signature. Whereas such models exist for several types of cancer including colorectal carcinoma, pancreatic carcinoma, squamous cell carcinoma, hepatocellular carcinoma, and lung cancer [18–22], none exist thus far for NB.

Ongoing studies in our laboratory deal with site-specific metastasis of NB and focus on the cross talk between these tumor cells and components of their microenvironment and on the downstream effects of such interactions. To facilitate such studies, we set out to develop an orthotopic mouse model for human NB metastasis. The orthotopic implantation of the SH-SY5Y and MHH-NB-11 human NB cell lines into the adrenal gland of nude mice yielded local tumors as well as lung metastases. This study describes the *in vivo* establishment of local tumor and metastatic variant lines from these tumors and their initial characterization.

Materials and Methods

Animals

Male athymic nude mice (BALB/c background) were purchased from Harlan Laboratories Limited (Jerusalem, Israel). The mice were housed and maintained for approximately 6 months in laminar flow cabinets under specific pathogen-free conditions in the animal quarters of Tel-Aviv University and in accordance with current regulations and standards of the Tel-Aviv University Institutional Animal Care and Use Committee. The mice were used in accordance with institutional guidelines when they were 7 to 10 weeks old.

Human NB Cell Lines and Culture Conditions

The SH-SY5Y [23] cell line was purchased from the American Type Culture Collection (Rockville, MD), and the MHH-NB-11 [24] cell line was kindly provided by Dr. T. Pietsch, Department of Neuropathology, University of Bonn Medical Center, Bonn, Germany. All human NB cells were maintained as monolayer cultures in growth medium: RPMI 1640 medium supplemented with 10% fetal calf serum (FCS), 100 U/ml streptomycin, 12.5 U/ml nystatin, 100 U/ml penicillin, and 2 mM L-glutamine (all materials were purchased from Biological Industries, Beit Ha'emek, Israel). The cultures were incubated at 37°C in a mixture of 6.5% carbon dioxide. The cultures were tested and found to be free of *Mycoplasma*. The cultures were maintained for no longer than 9 weeks after recovery from frozen stocks.

Orthotopic Inoculation of Tumor Cells

For *in vivo* inoculation, cells were harvested and transferred to RPMI 1640 medium supplemented with 5% FCS. Only single-cell suspensions of greater than 90% viability (trypan blue exclusion) were used for injection.

Anesthesia was induced by ketamine (100 mg/kg body mass; Kepro Deventer, The Netherlands) and 2% xylazine (10 mg/kg body mass; Medical Market, Tel Izhak, Israel) administered intraperitoneally. Tumor cells (1×10^6/50 μl) were injected orthotopically into the adrenal gland. This injection required surgical exposure of the left adrenal gland under anesthesia. Briefly, a left-side high-paracostal approach to the abdomen allowed visualization of the cranial tip of the left kidney. A 27-gauge needle was introduced through the left adrenal fat pad into the adrenal gland after retraction of the left kidney. The skin was closed by surgical stitching.

Necropsy Procedure and Histopathologic Studies

Mice were killed, and local (adrenal) tumor, lung, sternum, and other peritoneal organs suspected to hold metastases were harvested.

Lung and sternum were fixed in 4% buffered formalin (Bio-Lab Ltd., Jerusalem, Israel), embedded in paraffin, and sectioned. Sections were stained with hematoxylin and eosin and were evaluated by light microscopy for the presence of metastases.

In Vivo *Generation of Metastatic Variants from SH-SY5Y and MHH-NB-11 Human NB Cell Lines*

SH-SY5Y or MHH-NB-11 cells (1×10^6) were injected into the adrenal gland of nude mice. Local adrenal tumors, which appeared at the site of inoculation as well as in organs such as liver, bone marrow, and lung, suspected to harbor metastases were harvested, minced to pieces, and cultured *in vitro*. Primary cultures were passaged *in vitro* for three to five times. Cells harvested from these cultures were injected into the adrenal gland of another set of nude mice.

In the first *in vivo* cycle, NB cells were isolated from local adrenal tumors (designated as SY5Y.Ad or MHH.Ad cell variants) as well as from lung. Isolated NB cells from the lung were reinjected into the left adrenal gland of another set of nude mice. The inoculation of NB cells from the adrenal gland to lung was repeated two and three times to yield cell variants designated as SY5Y.Lu2 and MHH.Lu3, respectively.

Antibodies

The following antibodies were used for flow cytometry: phycoerythrin-conjugated mouse anti–human CD56 mAb (DakoCytomation, Glostrup, Denmark); rabbit anti–human CX3CL1 polyclonal antibody, 1 μg/sample (Torrey Pines Biolabs, Inc., East Orange, NJ); rabbit anti–human CX3CR1 polyclonal antibody, 1 μg/sample (eBioscience, San Diego, CA); anti–human CXCR3 mAb, 2.5 μg/sample (clone 49801), anti–human TrkA mAb, 0.25 μg/sample (clone 165131), anti–human TrkB mAb, 0.25 μg/sample (clone 72509), anti–human MRP1 mAb (clone QCRL; all from R&D, Systems Inc., Minneapolis, MN); anti–human CD44 polyclonal antibody, 0.25 μg/sample (BioLegend, San Diego, CA); and anti–human CXCR4 mAb, 0.5 μg/sample (CD184, clone B-R24; Diaclone, Stamford, CT). Anti–HLA-A, -B, and -C mAb (W6/32) [25] and anti–H-2 mAb (20-8-4S) [26] were kindly provided by Dr. R. Ehrlich, Department of Cell Research and Immunology, Tel-Aviv University, and were used at the dilutions of 1:500 and 1:3000, respectively, for flow cytometry. Fluorescein isothiocyanate (FITC)–conjugated goat antimouse IgG and goat antirabbit IgG (Jackson ImmunoResearch

Laboratories, West Grove, PA) were used at the dilution of 1: 50 as secondary antibodies for flow cytometry.

Affinity-purified goat anti–human hypoxia-inducible factor 1 alpha (HIF-1α) polyclonal antibody (R&D Systems, Inc.) and anti–human ERK 2 polyclonal antibody (Santa Cruz Biotechnology, Inc., Santa Cruz, CA) were used for Western blot analysis at the dilution of 1:1000. The anti–human matrix metalloproteinase 2 (MMP-2) mAb and anti–human MMP-9 mAb were used for Western blot analysis at 1 μg/ml (EMD Chemicals, Inc., San Diego, CA). Horseradish peroxidase–conjugated goat antimouse antibodies and rabbit antigoat antibodies were used according to the manufacturer's instructions (Jackson ImmunoResearch Laboratories).

Flow Cytometry

Double staining. For the double staining procedure, the cells ($0.5–1 \times 10^6$) were washed with FACS medium (RPMI 1640 supplemented with 5% FCS and 0.01% sodium azide). The samples were incubated for 1 hour at 4°C with the relevant primary antibody. After a wash with FACS medium, the cells were incubated for 1 hour at 4°C with FITC-conjugated secondary antibody. After another wash with medium, the cells were incubated for 1 hour at 4°C with a relevant antibody (conjugated with phycoerythrin). After an additional wash, antigen expression was determined using FACSort (Becton Dickinson, Mountain View, CA) and CellQuest software. Baseline staining was obtained by labeling the cells with secondary antibodies alone.

Single staining. Neuroblastoma cells were cultured for 24 hours in growth medium containing 10% FCS. Cells ($0.5–1 \times 10^6$) were incubated for 1 hour at 4°C with relevant primary antibody. After a wash with FACS medium, the cells were incubated for 1 hour at 4°C with FITC-conjugated secondary antibody. After an additional wash, antigen expression was determined using Becton Dickinson FACSort and CellQuest software. Baseline staining was obtained by labeling the cells with secondary antibodies alone. For intracellular staining of MRP-1, cells were incubated with absolute methanol at −20°C for 30 minutes and then rinsed twice with FACS medium before the staining procedure. Statistical analysis was performed using Student's *t* test.

Cytogenetic Analysis

Chromosome spreads were prepared according to conventional cytogenetic techniques. Multiplex fluorescence *in situ* hybridization analysis for 24-color karyotyping was performed according to the manufacturer's protocols (Meta Systems GmbH, Altlusshein, Germany). Multiplex fluorescence *in situ* hybridization signals were visualized using a fluorescence microscope (AxioImager Z.1; Zeiss, Göttingen, Germany) and analyzed using Isis-366 software.

Wound Healing Assay

The wound healing assay was performed in cells growing in 24-well plates coated with 5 to 10 μg/ml fibronectin (Biological Industries). Upon confluency, the cell monolayer was wounded with a plastic tip, then washed twice with RPMI medium, and replaced with a fresh growth medium. Closure of the denuded area was monitored using an inverted microscope (Eclipse TE 2000-S; Nikon, Enfield, CT) fitted with a digital camera (DXM1200F; Nikon). Photo documentation was taken at days 1, 2, 3, and 4 after the wounding.

Hypoxia Mimetic Assay

Neuroblastoma cells (2×10^6) were plated in growth medium. After an overnight incubation, the medium was replaced with fresh growth medium supplemented with 0, 25, and 50 μM deferoxamine mesylate salt (DFX; Sigma, St. Louis, MO). After 24 hours of incubation, nonadherent and adherent cells were pelleted and lysed with RIPA buffer [20 mM Tris, pH 8, 150 mM NaCl, 1% NP-40 (Sigma), 0.1% SDS, 0.75% deoxycholate, 5 mM EDTA, pH 8, 3 mM EGTA, pH 8, 20 mM sodium phosphate, pH 7.6, 2 mM sodium orthovanadate, 5 mM NaF, 5 mM sodium pyrophosphate, pH 7.6, 2 ng/ml aprotinin, 2 ng/ml leupeptin, and 1 mM PMSF (Sigma)]. Samples were used for the detection of HIF-1α by Western blot analysis.

Gelatin Substrate Zymography

Neuroblastoma cells were plated in growth medium. The growth medium was removed after overnight incubation and was replaced by serum-free RPMI for an additional 24 hours. Matrix metalloproteinases production in the conditioned medium was determined by separation on 7.5% SDS–polyacrylamide gels (PAGE) containing 0.1% gelatin substrate. After electrophoresis, gels were washed three times in 50 mM Tris–HCl, pH 7.4, containing 2.5% Triton X-100. The gels were then washed three times in 50 mM Tris–HCl buffer, pH 7.4, followed by incubation in an incubation buffer, consisting of 50 mM Tris–HCl, pH 7.4, 0.02% sodium azide, and 10 mM $CaCl_2$ for 48 hours at 37°C. After three washes in double-distilled H_2O, the gels were stained with 0.25% Coomassie blue and destained in 20% methanol and 10% glacial acetic acid, and then clear bands of protein degradation were visualized.

Western Blot Analysis

Conditioned medium samples that were used in the gelatin substrate zymography assay were resolved on SDS-PAGE and transferred onto a 0.45-μm polyvinylidene fluoride membrane (Millipore, Bedford, MA). For the hypoxia mimetic assay, cell lysates were incubated for 15 minutes on ice and cleared by centrifuging at 16,000*g* for 20 minutes at 4°C. After the addition of Laemmli sample buffer, the lysates were boiled for 10 minutes, resolved on SDS-PAGE, and transferred onto nitrocellulose membrane. After the transfer, the membrane was incubated at room temperature with 5% dry milk in TBS–Tween for 1 hour to block free binding sites on the membrane. The proteins of interest were detected by specific antibodies. The proteins were visualized on film using ECL (Amersham Pharmacia Biotech, Buckinghamshire, England).

Proliferation In Vitro *and Viability Assays*

Neuroblastoma cells were harvested from 80% confluent monolayer cultures. The cells were seeded at a density of 1×10^4 to 10^5 cells per well in a 96-well flat-bottomed tissue culture plate. After 24 hours of incubation, the indicated concentrations of doxorubicin hydrochloride, Dox (Sigma), or DFX were added to the wells. Proliferation and viability under normal conditions or after Dox treatment were monitored in quadruplicates after 0, 24, 48, 72, and 96 hours with an XTT-based assay according to the manufacturer's instructions (Biological Industries). Cell proliferation after DFX treatment was estimated in duplicates after 24 hours using the XTT assay. Absorbance at 450 nm (OD_{450}) was determined for each well using

an automated microplate reader (SpectraMax 190; Molecular Devices Corp., Sunnyvale, CA), and subtraction of nonspecific readings (measured at 630 nm) was done automatically during the OD_{450} reading. To obtain the percentage of cell growth or cell viability, the OD_{450} of the cells (in each time point of Dox treatment) was divided by the OD_{450} of the cells at the initial time point of the experiment. For DFX-treated cells, percentage of cell viability was calculated by dividing the OD_{450} of these cells by OD_{450} of the untreated cells.

Statistical Analysis

Unpaired Student's *t* test was used to compare *in vitro* results. Survival analysis was computed by the Kaplan-Meier method and compared by the log-rank test. Fisher's exact test was used to compare number of mice with lung metastasis.

Results

Generation of Local and Metastatic NB Variants

It was previously demonstrated that orthotopic inoculation of NB cells produces a more relevant model than a heterotopic inoculation [14]. The orthotopic NB model has the advantage of reflecting more accurately the biology of the local primary tumor and of the metastases including the interactions of the tumor cells with their microenvironment. Similar interactions occur in pediatric patients with adrenal NB [14].

Neuroblastoma cells from the SH-SY5Y or MHH-NB-11 cell lines were injected into the left adrenal gland of athymic nude mice. The animals were examined weekly, and laparotomy was performed when animals showed terminal signs (swelling of the abdomen, protrude left adrenal tumor, and reduced body mass).

The local tumors were harvested to yield the local variants: SY5Y.Ad and MHH.Ad. Lung metastases were harvested from lungs of tumor-bearers and reestablished in culture. Cells from these cultures were reinjected into the adrenal gland of another set of athymic nude mice. After two to three such inoculation cycles, the metastatic variants SY5Y.Lu2 and MHH.Lu3 were established in culture (Figure 1).

To determine whether the isolated variants had increased metastatic potential, cells from the local and the metastatic variants were inoculated orthotopically into nude mice. Histopathology detected lung metastases in 5 of 8 mice inoculated with the metastatic variant SY5Y.Lu2 and in 5 of 11 mice inoculated with the metastatic variant MHH.Lu3. None of the local variants produced lung metastases in the injected mice (Table 1). Bone marrow metastases were not detected by histopathology.

Preliminary data showed that inoculation of SY5Y.Lu2 and MHH.Lu3 into the adrenal gland of nude mice produced lung and bone marrow micrometastases (detected by the successful isolation of tumor cells from the lung and bone marrow of tumor-bearing mice).

The original SH-SY5Y or MHH-NB-11 cell lines, as well as the local and the metastatic variants from these lines, were tested for their aggressiveness (i.e., the time interval during which a given inoculum of cells kills the host). The cells were injected into the adrenal gland of nude mice, and the mice were killed when moribund (63–247 days after inoculation). All cell variants were tumorigenic after orthotopic inoculations (Table 1). The median survival time after the intra-adrenal injection of SH-SY5Y, SY5Y.Ad, or SY5Y.Lu2 cells was 116, 109, and 80 days, respectively (Figure 2*A*). The median survival time after the intra-adrenal injection of MHH-NB-11, MHH.Ad, or MHH.Lu3 cells was 139, 110, and 86 days, respectively (Figure 2*B*). These results demonstrate that *in vivo* passaged tumor cells are more aggressive than the corresponding cultured ones confirming previous studies [27] and that the metastatic variants are more aggressive than the corresponding local tumor variants.

Characterization of Local and Metastatic NB Variants

Immunophenotyping and karyotyping of local and metastatic variants of NB. We next phenotyped the local and metastatic variants with double-color flow cytometry. All of the variants strongly expressed human CD56 [28], HLA class I, and did not express mouse H-2 class I (Figure 3). These results confirmed the identity of the tumor variants as human NB cells.

The variants were analyzed with a broad panel of antibodies against cell surface antigens by flow cytometry. The local and the metastatic variants of both the SH-SY5Y and the MHH-NB-11 systems showed a similar expression pattern of the NB prognostic antigens TRK A, TRK B, CXCR4, CD44, and MRP-1 [2]. Similar results were obtained with CX3CL1, CX3CR1, and CXCR3. These chemokines and chemokine receptors represent markers that may be relevant to NB progression [29] (Nevo et al., unpublished observations).

A cytogenetic study did not detect differences between the local and metastatic variants of the MHH tumor in structural chromosomal rearrangements, including in homogeneously staining regions representing genomic amplification of MYCN and t(1;17) translocations (Figure W1). This indicated that no additional chromosomal aberrations were acquired by the metastatic variant beyond those that existed in the local variant.

Differential drug sensitivity of local and metastatic variants of NB. The local and the metastatic variants as well as the parental cell lines did not differ in their proliferative capacity *in vitro* under normal culture conditions (in serum-containing medium).

We next analyzed the viability of the cell variants in the presence of Dox, a chemotherapeutic agent commonly used in the treatment of NB [30]. MHH.Ad and MHH.Lu3 were cultured in the presence of 1 μM Dox for up to 96 hours. As expected, the MHH.Lu3 metastatic variant exhibited a significantly higher resistance to Dox than the local variant. After 48 hours of exposure to Dox, the average cell viability was 19 ± 7% and 55 ± 6%, respectively ($P < .001$). This effect was more pronounced with 1 μM than with 0.5 μM Dox.

Because 1 μM Dox caused a massive cell death in both SY5Y variants, we decreased the concentration of Dox to reveal a differential drug sensitivity of local and metastatic variants if existing. SY5Y.Ad and SY5Y.Lu2 variants were cultured in the presence of 0.125 μM Dox for up to 96 hours. In contrast to the MHH variant system, Dox was significantly more toxic to the metastatic variant than to the local variant (higher concentrations of Dox were toxic to both of the variants). The average cell viability after 48 hours was 57 ± 6% for the local variant and 20 ± 11% for the metastatic variant ($P < .05$). Similar results were obtained after 24 hours of exposure to Dox.

Deferoxamine, an iron chelator, is a hypoxia mimetic agent that up-regulates HIF-1α and certain inflammatory mediators. Deferoxamine was shown to exhibit antiproliferative properties in human NB cell lines [31,32]. Deferoxamine alone, or in combination with

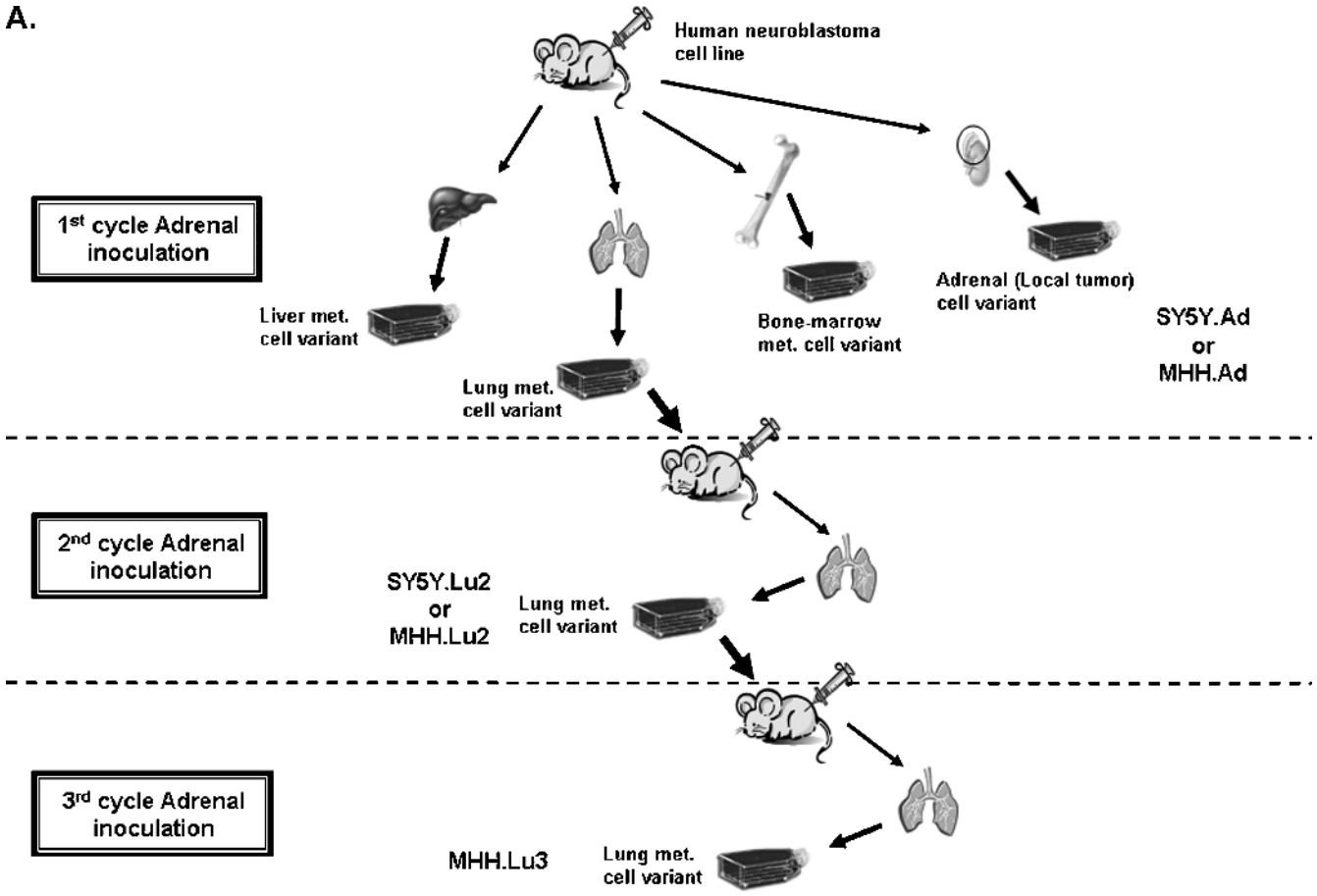

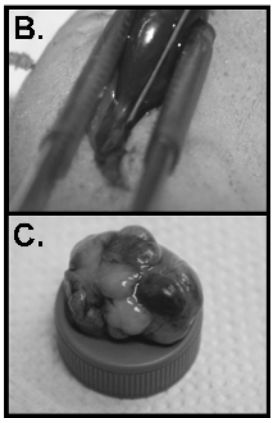

D.

	SH-SY5Y system	MHH-NB-11 system
Parental cell-line	SH-SY5Y	MHH-NB-11
local tumor variant	SY5Y.Ad	MHH.Ad
Metastatic variant	SY5Y.Lu2	MHH.Lu3

Figure 1. The *in vivo* generation of local and metastatic human NB variants. (A) Neuroblastoma cells from the SH-SY5Y or MHH-NB-11 cell lines were injected into the left adrenal gland of athymic nude mice. The local tumors, SY5Y.Ad and MHH.Ad, were harvested and established in culture. Lung metastases were harvested, and tumor cells were reinjected into the adrenal gland of another set of athymic nude mice. The cycles were repeated one or two additional times to yield the metastatic variants, SY5Y.Lu2 and MHH.Lu3, respectively. (B) Orthotopic injection of NB cells into the left adrenal gland, as described in the Materials and Methods section. (C) A local (adrenal) tumor harvested from a xenografted mouse. The local tumors in most of the animals were bulky and surrounded the left kidney. (D) Parental cell lines, local and metastatic variants used in this study.

other cytotoxic agents, is often used as an antiproliferative agent in patients with NB [33,34].

The SY5Y.Ad, SY5Y.Lu2, MHH.Ad, and MHH.Lu3 variants were cultured in the presence of 0, 25, 50, and 100 μM DFX for 24 hours. The MHH metastatic variant displayed significant resistance to DFX compared to the corresponding local variant. The average cell viability was obtained as described in the Materials and Methods section. The viability of the local variant cells was 90 ± 10% (25 μM DFX), 80 ± 15% (50 μM DFX), and 76 ± 8% (100 μM DFX) compared to 119 ± 7% (25 μM DFX; $P < .01$), 119 ± 12% (50 μM DFX; $P < .05$), and 106 ± 16% (100 μM DFX; $P < .05$) of the viable cells in the metastatic variant.

Table 1. Tumorigenicity and Metastasis Formation in Nude Mice by Local and Metastatic Human Neuroblastoma Variants.

Variant	% Mice with Adrenal Tumors (Orthotopic)	No. Mice with Lung Metastasis*	Fisher's Exact Test, *P*	No. Mice with Bone Marrow Metastasis*
SY5Y.Ad	100	0/6		0/7
SY5Y.Lu2	100	5/8	0.03†	0/9
MHH.Ad	100	0/12		0/7
MHH.Lu3	100	5/11	0.01‡	0/11

Nude mice were injected into the adrenal gland with 1×10^6 cells. The mice were killed when moribund and necropsied. The presence of local (adrenal) tumor was determined.
Lung and sternum sections were stained with hematoxylin and eosin and evaluated by light microscopy for the presence of metastases.
*Number of tumor-positive mice per number of inoculated mice.
†*Versus* SY5Y.Ad.
‡*Versus* MHH.Ad.

Similar results were obtained with the SY5Y variants (data not shown). Overall, DFX was toxic to both local variants but not to the metastatic variants.

Morphology and migratory capacity of local and metastatic variants of NB. Figure 4, *A* and *B*, demonstrates that the local and the metastatic variants of both the SH-SY5Y and MHH-NB-11 cells present distinct cell morphologies. The local variants resemble the cultured parental cell lines. These cells have a neuroblastic phenotype, a small, round cell body that may have short neuritic processes and grow as poorly attached aggregates. In contrast, the metastatic variants are morphologically flattened, moderately adherent with relatively long neuritic processes that are growing mostly in monolayer.

Enhanced cell migration is associated with and leads to metastasis. Therefore, we compared the migratory ability of the local and the metastatic variants. The wound healing assay showed that after 24 to 72 hours, the metastatic SY5Y.Lu2 variant had a significantly higher rate of wound closure compared to the local variant (Figure 4*C*).

Figure 4*D* demonstrates that in the MHH.Lu3 metastatic variant, there is a population of cells that migrated into the gap already after 24 hours. This population continued to migrate into the gap in the next 48 hours of the experiment. This migratory cell population was absent in the local MHH.Ad variant. The closure of the wound by these cells after 72 hours seems to be due to cell proliferation and not to increased motility.

Secretion of MMP-2 and MMP-9 from local and metastatic variants of NB. Matrix metalloproteinases are a phenotypic characteristic of malignant cancer cells that function as promalignancy factors. These tumor-derived enzymes support the invasion of tumor cells through the basement membrane [35]. Matrix metalloproteinases antagonize apoptosis, orchestrate angiogenesis, and regulate innate immunity, resulting in tumor dissemination and metastasis [36].

Gelatin zymography was used to determine the activity of gelatinases (MMP-2 and MMP-9) in the cell variants. It was shown that the metastatic variant SY5Y.Lu2 displayed a relatively higher activity level of the two gelatin-degrading enzymes (~66 and ~92 kDa) than the parental SH-SY5Y cells and the local SY5Y.Ad variant. All the cell variants of the MHH system produced only the ~66-kDa enzyme at a similar level of activity (data not shown). Using antibodies directed against MMP-2 and MMP-9, we identified the above proteolytic enzymes as the active form of MMP-2 and the proMMP-9.

Expression of HIF-1α by local and metastatic variants of NB. Hypoxia, a common feature of solid tumors, exerts gene regulatory activities and selective pressures on tumor cells that drive their progression. Oxygen homeostasis is predominantly controlled by the transcriptional activator HIF-1 within the cell. Whereas the beta subunit of this heterodimeric factor is oxygen-independent, the alpha subunit HIF-1α is stable and active only in the absence of oxygen [37]. Under hypoxia, HIF induces or represses numerous genes that control multiple cell functions involved in tumor growth, progression, invasion, and metastasis [38]. As mentioned previously, DFX is an iron chelator that up-regulates HIF-1α and thus mimics hypoxia conditions in culture [31,32].

To determine whether HIF-1α is differentially expressed in the local and the metastatic variants of NB, we treated the cells with 0, 25, and 50 μM DFX for 24 hours and analyzed HIF-1α protein expression using Western blot analysis. As shown in Figure 5, 25 or 50 μM of DFX induced an increase of HIF-1α expression in all the variants. At both concentrations of DFX, the expression of HIF-1α was higher in the metastatic variants of the SY5Y and MHH systems compared to the corresponding local variants.

Because HIF-1α confers on cells the ability to cope with hypoxic stress [37], it is expected that the metastatic variants would more readily up-regulate the expression of HIF-1α than the nonmetastatic ones when exposed to hypoxia mimetic conditions.

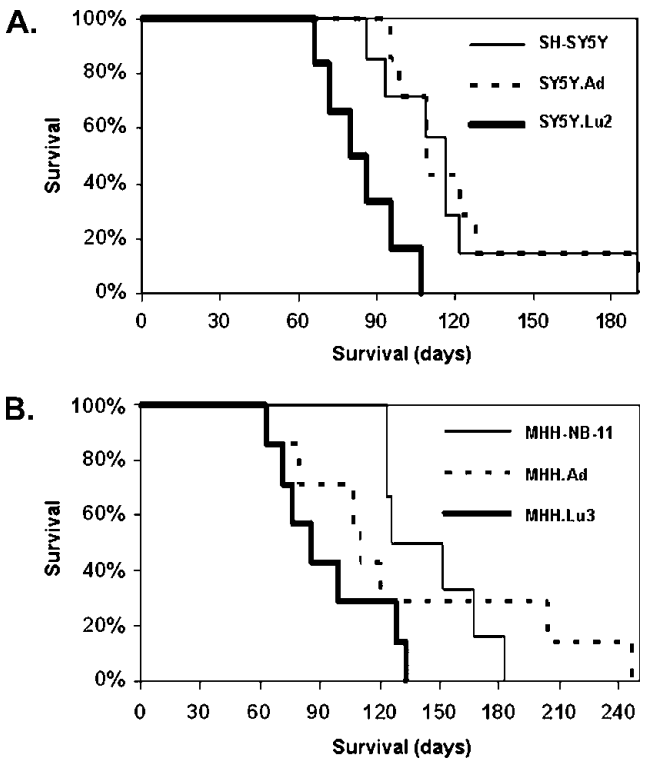

Figure 2. Survival curves of nude mice bearing local and metastatic variants of NB. Local and metastatic variants of NB were inoculated orthotopically into the adrenal gland of nude mice. Kaplan-Meier survival curve shows that the survival of mice bearing the metastatic variant: SY5Y.Lu2 (A) or MHH.Lu3 (B) was significantly shorter than that of mice bearing tumors generated by the corresponding local variant or the parental cell line. (Log-rank statistic: SH-SY5Y *versus* SY5Y.Lu2, $P < .01$; SY5Y.Ad *versus* SY5Y.Lu2, $P < .01$; MHH-NB-11 *versus* MHH.Lu3, $P < .05$).

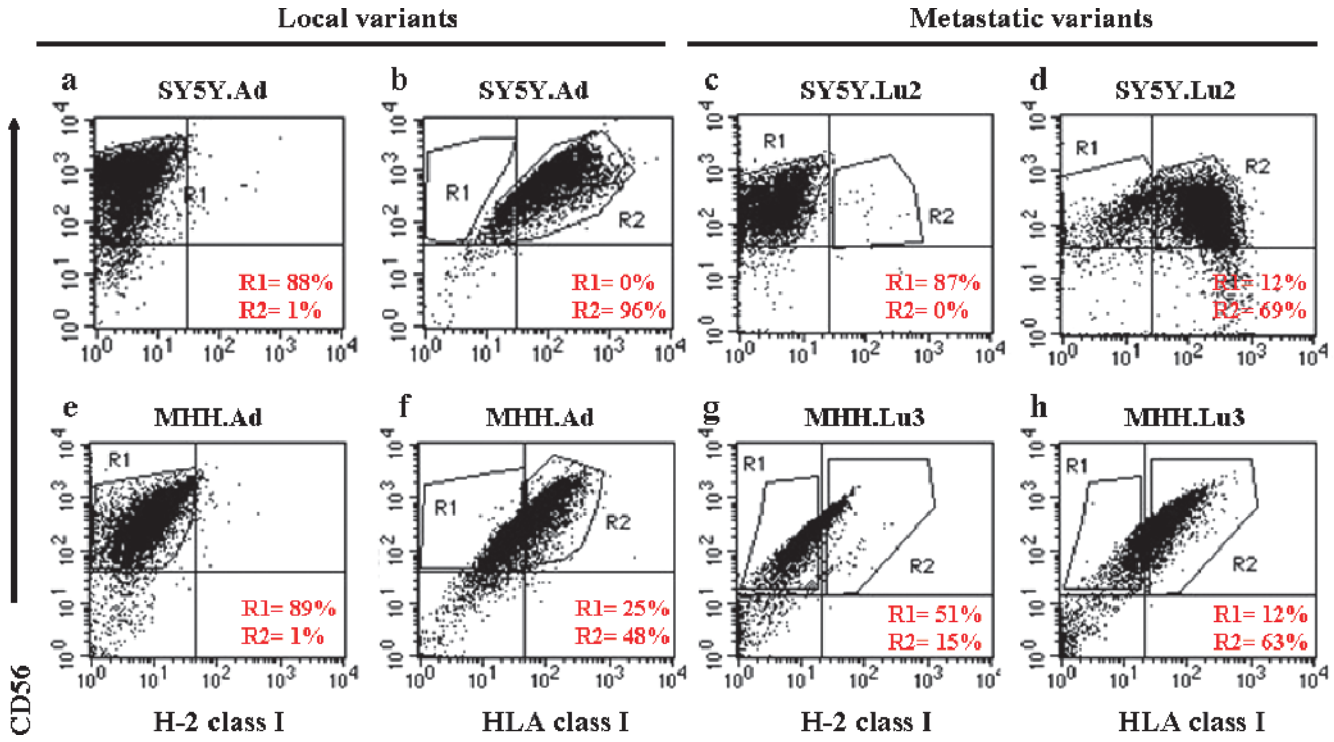

Figure 3. Immunophenotyping of local and metastatic NB variants. Flow cytometric analyses of the NB local variants, SY5Y.Ad (a, b) and MHH.Ad (e, f), and the NB metastatic variants, SY5Y.Lu2 (c, d) and MHH.Lu3 (g, h), using monoclonal antibodies against CD56/HLA/H-2. Cells were positive for HLA and CD56 but negative for H-2. Percentages of $CD56^+/HLA^+/H\text{-}2^-$ were calculated by using the following gating strategy. On a FL1-H/FL2-H dot plot, the $CD56^+/H\text{-}2^-$ cells were identified by region R1. In a second dot plot, region R1 was defined $CD56^+/H\text{-}2^-$, and region R2 was used to identify the $CD56^+/HLA^+$ human NB cells.

The association between increased HIF-1α expression and increased metastatic potential is supported by clinical correlation between increased HIF-1α expression and increased patient mortality in several types of cancer [39].

Discussion

Metastasis develops when genetically unstable cancer cells adapt to a tissue microenvironment that is distant from the primary tumor. The metastatic process involves several sequential, interrelated, and rate-limiting inductive and selective steps. It exploits both the selection of intrinsic beneficial properties of tumor cells and the simultaneous recruitment of host microenvironmental properties that support invasion, angiogenesis, and other promalignancy functions of metastatic tumor cells [11]. Thus, metastasis can be described as a process that emerges from the somatic evolution of a genetically diversified cancer cell population under the selective pressures of an environment that imposes tight rules on cell behavior [9].

The generation of tumor cell populations that differ in their metastatic ability is a gradual process, requiring several cycles of *in vivo* passages, as was shown previously in several studies [20,27,40].

Neuroblastoma tumors are heterogeneous tumors derived from the neural crest [41]. Metastasis is the leading cause of death of NB patients, and despite substantial recent progress [10], we still have to broaden our understanding of NB metastasis.

Neuroblastoma disseminates most frequently to bone marrow (87%) and to bone (66%) [4,5,41]. Neuroblastoma pulmonary metastases are rare at diagnosis and represent a terminal stage [6–8,41]. Kammen et al. [8] reported that although some NB patients with lung metastasis responded to treatment, all patients died of relapse in the lung or of progressed lung disease.

These data compelled us to focus specifically on lung metastasis that may reflect more biologically aggressive cells and portends a poor prognosis.

The cellular and molecular events leading to NB metastasis are largely unexplored. One of the reasons for this is the lack of relevant and reliable human xenograft animal models. In this study, we filled this gap by developing an *in vivo* model for NB metastasis, thereby providing an unlimited source for cells representing local and metastatic NB. This model is a critical tool for future studies on NB metastasis.

We describe the generation and characterization of two novel human NB xenograft models, each comprising a local tumor variant and a lung metastatic variant. Two NB cell lines were used to develop these variants: the SH-SY5Y cell line, a subclone derived from the SK-N-SH cell line that was established from a bone marrow biopsy, and the MHH-NB-11 cell line, derived from a tumor mass involving the adrenal gland [23,24]. Cells from both lines were injected orthotopically into the adrenal gland of nude mice. The local encapsulated tumor and lungs suspected of containing metastatic lesions were harvested, and the tumor cells were recovered in culture. Lung metastatic tumor cells were then reinjected into the adrenal gland of another set of nude mice. After two to three inoculation cycles, we established local tumor variants and lung metastatic variants of both NB cell lines.

By using this procedure, we probably induced a metastatic phenotype in the originally nonmetastatic MHH tumor and increased the metastatic phenotype of the SY5Y tumor.

The human NB nature of the cells was confirmed by a strong positive expression for human CD56 [28], and HLA class I and by lack of expression of mouse H-2 class I.

The phenotype and the behavior of the metastatic variants were compared to those of the local tumor variants. All the variants were tumorigenic after an orthotopic injection into the adrenal gland of nude mice. The SY5Y.Lu2 variant, which was derived after two transplantation cycles *in vivo*, produced lung metastasis in 60% of inoculated mice, and the MHH.Lu3, derived after three transplantation cycles *in vivo*, produced lung metastasis in 45% of inoculated mice. The local variants from both tumor systems did not produce metastasis.

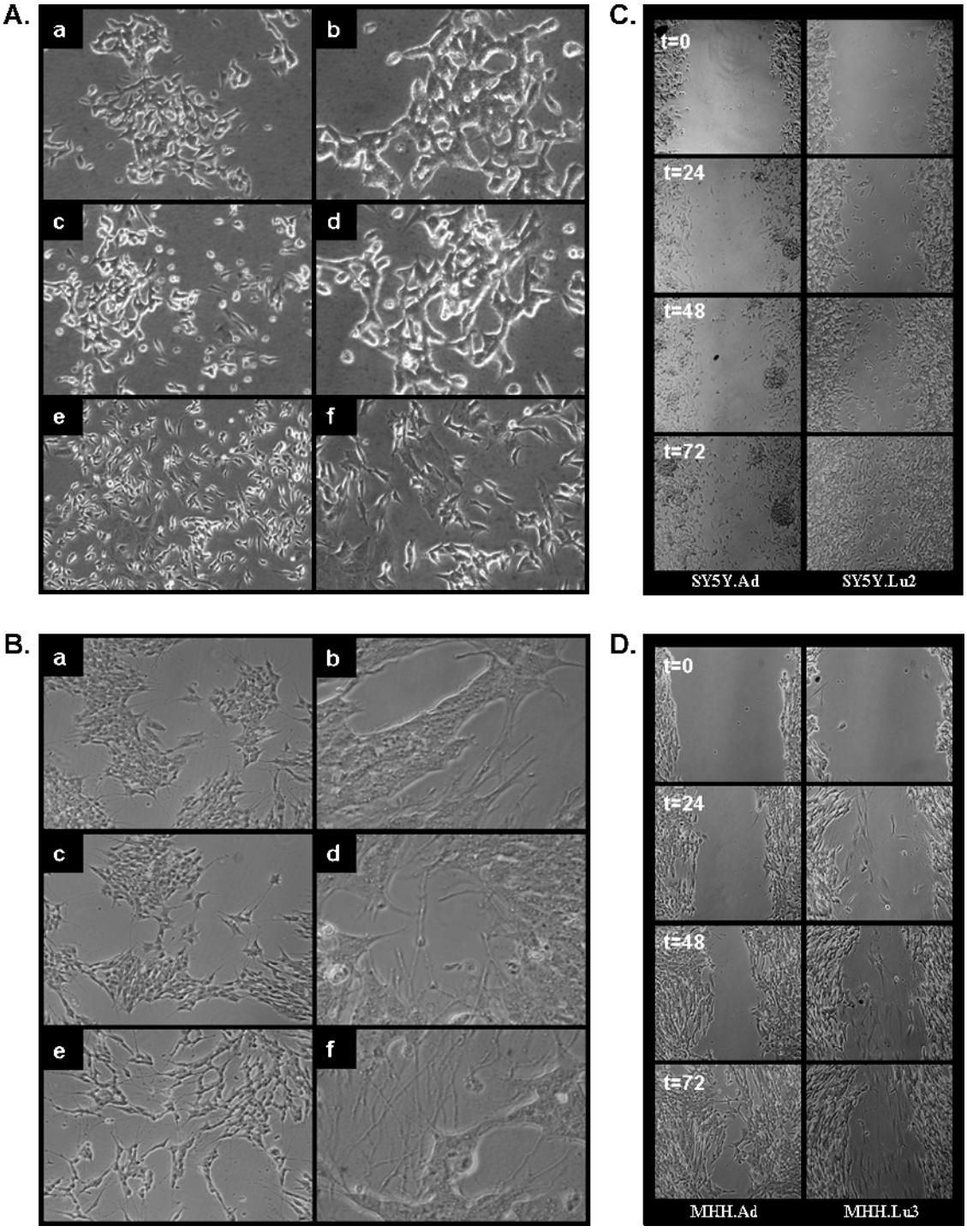

Figure 4. Distinct cell morphologies and migratory capacity of local and metastatic NB variants *in vitro*. Morphology of (A) SH-SY5Y (a, b), SY5Y.Ad (c, d), and SY5Y.Lu2 (e, f). Morphology of (B) MHH-NB-11 (a, b), MHH.Ad (c, d), and MHH.Lu3 (e, f). Phase contrast photomicrographs: a, c, and e original magnification, ×10; b, d, and f original magnification, ×40. Phase contrast photomicrographs of scratched monolayers in a wound healing assay: SY5Y.Ad and SY5Y.Lu2 variant cells (C) and MHH.Ad and MHH.Lu3 variant cells (D) at 0, 24, 48, and 72 hours. Shown are representative photomicrographs (original magnification, ×10) of two to three independent experiments.

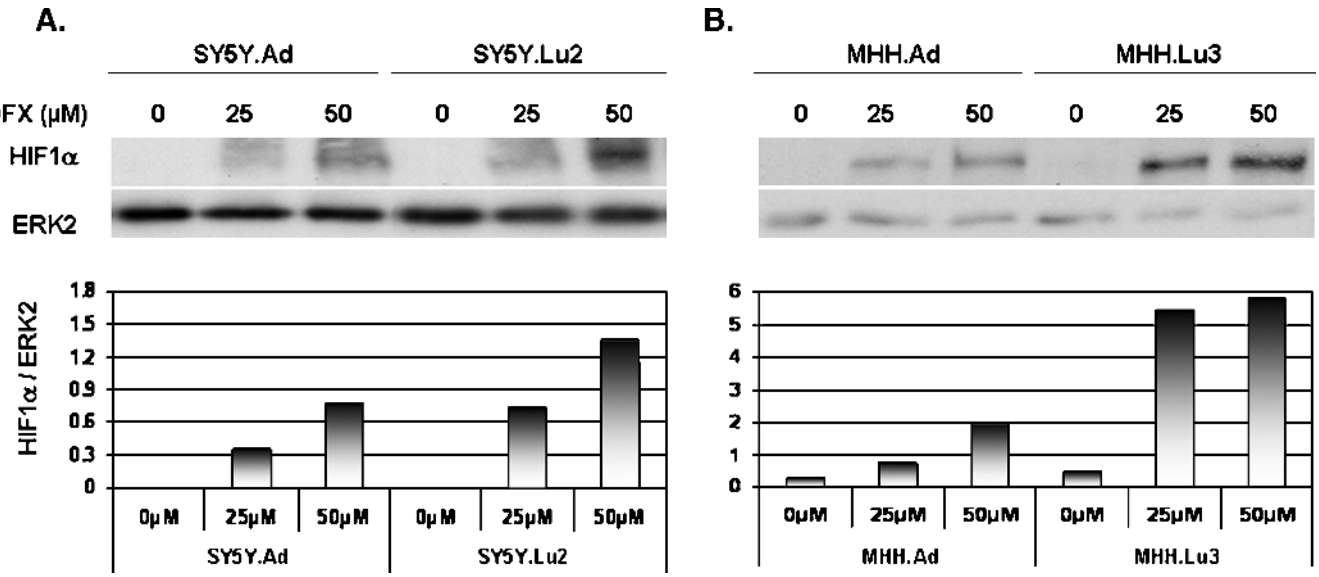

Figure 5. Induction of HIF-1α in local and metastatic NB variants by the hypoxia mimetic DFX. (A) SY5Y.Ad and SY5Y.Lu2 variant cells and (B) MHH.Ad and MHH.Lu3 variant cells were treated with 0, 25, and 50 μM DFX for 24 hours. HIF-1α and ERK2 (loading control) expression was detected by Western blot analysis. Presented are the results of one representative blot and its densitometry analysis of four independent experiments.

Although the SY5Y.Lu2 and MHH.Lu3 variants did not produce bone marrow metastases, ongoing experiments indicate that the orthotopic inoculation of these variants into the adrenal gland of nude mice produced bone marrow micrometastases in the inoculated mice. The presence of micrometastases, which might escape morphologic identification during the histopathologic analysis, suggests that tight microenvironmental conditions in murine bone marrow can suppress the formation of NB macrometastases at this site.

The metastatic variants were flattened with relatively long neuritic processes, were moderately adherent, and mostly grow as monolayers. Morphologically, these cells resemble the human NB intermediate-type (I-type) cells, which exhibit biochemical features of both neuroblastic (N) cells and substrate-adherent (S) cells [42,43]. Neuroblastoma I-type cells are multipotent embryonic precursor cells of the peripheral nervous system. We postulated, therefore, that similar to these cells, the metastatic variants are highly tumorigenic and are capable of self-renewal, proliferation, and further differentiation [42].

Whereas the proliferative capacity of the local and the metastatic variants was essentially identical under normal culture conditions, these variants differ in their sensitivity to the apoptosis-inducing agent doxorubicin.

Keshelava et al. [44] demonstrated that chemotherapeutic agents given to NB patients can confer an *in vivo* selection pressure, which leads to resistance to cytotoxic drugs. However, because both the MHH-NB-11 and the SH-SY5Y cell lines were established from NB patients that showed no response to chemotherapy, this cannot explain our results [24,45].

Our findings, however, can be explained by Fidler's clonal paradigm indicating that metastatic lesions are not necessarily uniform with respect to certain biologic properties [46]. In this regard, Spengler et al. [47] demonstrated a differential drug sensitivity of two subclones (SH-SY5Y and SH-EP) derived from the human NB cell line SK-N-SH. Our study reveals that although the *in vivo*–generated NB metastatic variants expressed a metastatic phenotype, they exhibited a diverse response to doxorubicin. The question of whether the differential chemoresistance observed in this study is related to specific molecular or metabolic alterations associated with the *in vivo* procedure *per se* remains to be established.

Enhanced cell migration and increased proteolytic enzyme activity are promalignancy characteristics [48]. Our results indicate that the SY5Y metastatic variant migrated significantly faster and that its MMP-2 and MMP-9 activity was higher than the local variant. Indeed, increased activity of MMP-2 and MMP-9 has been reported to occur in patients with advanced NB [49,50]. Similar results were not obtained with the MHH cells. The possibility cannot be excluded that the repeated *in vivo* pressures (selection, adaptation, and induction) led to the isolation of a population of metastatic cells that express and release proteolytic enzymes, not tested in this work [35,51]. Such enzymes could contribute to their enhanced motility and invasion *in vivo* and *in vitro*.

Our previous study suggested that CXCR4 is involved in the formation of NB bone marrow metastases [52]. Expression of functional CXCR4 was further described to confer a distinct gene expression profile on neuroblastoma cells [53]. Tumor cells that arrive at their target organ are exposed to various factors expressed at this site. These factors promote or restrict their adhesion, invasion, and proliferation. Thus, the expression of functional receptors by the tumor cells that arrive at the metastatic site and the equilibrium between the corresponding factors may affect the fate of the metastatic process [29]. To further test this assumption, we tested the expression of several chemokine receptors in our variant systems. The local tumor cell variants as well as the metastatic variants were found to express similar levels of these receptors. The lack of difference in chemokine receptor expression between the metastatic and nonmetastatic variants can be explained by the results of Holland et al. [54]. A differential CXCR4-mediated chemotaxis was seen in a range of breast cancer cell lines covering a spectrum of invasive phenotypes, whereas the expression levels of CXCR4 were uniform across the entire panel, only highly invasive

cells expressed functional receptors [54]. In another study, Palmesino et al. [55] showed that B cells in all stages of maturation exhibit similar expression levels of CXCR4. However, mature B cells exhibit a reduced activity of this receptor. This reduction in activity could be the result of a biochemical mechanism [55]. We speculate that similarly to breast cancer cells and B cells, local and metastatic NB cells express similar levels of CXCR4, CX3CR1, and CXCR3 throughout the metastatic process but may express a differential functional activity of these receptors. Specific chemokine receptor–associated proteins or changes in glycosylation patterns may be responsible for the fine-tuning of receptor-mediated responses.

Hypoxia, a common characteristic of the microenvironment of solid tumors, activates HIF-1α, a transcription factor and a key element for several signaling pathways in hypoxic tissues as well as in tumor cells [37,38]. In this study, we demonstrated that under hypoxia mimetic conditions, the expression of HIF-1α in the metastatic variants was higher than its expression in the local variants. Thus, HIF-1α probably plays a significant role in conferring a high-malignancy phenotype on the SY5Y.Lu2 and MHH.Lu3 metastatic NB variants. This supports the results of previous studies showing that HIF-1α is a metastasis-regulating gene, and its activities are strongly linked to invasion, angiogenesis, and tumorigenesis [37,38]. Deferoxamine has been shown to induce the activity of HIF-1α in a manner similar to the induction of HIF-1 by hypoxia [56].

Although DFX functions as an antiproliferative agent for the treatment of NB patients [33,34], it can also function as a proinvasive factor [57]. Indeed, DFX-treated metastatic variants exhibited an increased proliferation capacity compared to DFX-treated local variants. Sullivan and Graham [58] suggested that the acquisition of the metastatic phenotype is not simply the result of disregulated signal transduction pathways but is achieved through a stepwise process driven by multiple hypoxia-inducible mechanisms, such as intravasation, motility, and extravasation. Furthermore, tumor cells in a hypoxic environment undergo adaptive changes that allow them to survive and proliferate.

Taken together, the establishment of a reproducible orthotopic model of human NB metastasis offers an unlimited source for material amenable for transcriptomic and proteomic analyses. The above data and the requisite of an effective NB treatment accentuate the need to concurrently understand the metastatic process as well as the phenotypic diversity of NB metastasis.

References

[1] National Cancer Institute, Surveillance, Epidemiology, and End Results Database. Available at: http://seer.cancer.gov. Accessed July 2007.

[2] Vasudevan SA and Nuchtern JG (2005). Gene profiling of high risk neuroblastoma. *World J Surg* **29**, 317–324.

[3] Brodeur GM (2003). Neuroblastoma: biological insights into a clinical enigma. *Nat Rev Cancer* **3**, 203–216.

[4] Brodeur GM and Castleberry RP (1997). Chapter 29. Neuroblastoma. In PA Pizzo and DG Poplack (Eds). Principles and Practice of Pediatric Oncology. Philadelphia, PA: Lippincott-Raven Publishers, pp. 761–783.

[5] Brodeur GM (1991). Chapter 24: Neuroblastoma and other peripheral neuroectodermal tumors. In DJ Fernbach and TJ Vietti (Eds.). Clinical Pediatric Oncology. Mosby Year Book, St, Louis, MO, pp. 437–464.

[6] Cowie F, Corbett R, and Pinkerton CR (1997). Lung involvement in neuroblastoma: incidence and characteristics. *Med Pediatr Oncol* **28**, 429–432.

[7] Towbin R and Gruppo RA (1982). Pulmonary metastases in neuroblastoma. *AJR Am J Roentgenol* **138**, 75–78.

[8] Kammen BF, Matthay KK, Pacharn P, Gerbing R, Brasch RC, and Gooding CA (2001). Pulmonary metastases at diagnosis of neuroblastoma in pediatric patients: CT findings and prognosis. *AJR Am J Roentgenol* **176**, 755–759.

[9] Gupta GP and Massague J (2006). Cancer metastasis: building a framework. *Cell* **127**, 679–695.

[10] Ara T and DeClerck YA (2006). Mechanisms of invasion and metastasis in human neuroblastoma. *Cancer Metastasis Rev* **25**, 645–657.

[11] Fidler IJ (2003). The pathogenesis of cancer metastasis: the "seed and soil" hypothesis revisited. *Nat Rev Cancer* **3**, 453–458.

[12] Witz IP (2008). Yin-yang activities and vicious cycles in the tumor microenvironment. *Cancer Res* **68**, 9–13.

[13] Beltinger C and Debatin KM (2001). Murine models for experimental therapy of pediatric solid tumors with poor prognosis. *Int J Cancer* **92**, 313–318.

[14] Khanna C, Jaboin JJ, Drakos E, Tsokos M, and Thiele CJ (2002). Biologically relevant orthotopic neuroblastoma xenograft models: primary adrenal tumor growth and spontaneous distant metastasis. *In Vivo* **16**, 77–85.

[15] Henriksson KC, Almgren MA, Thurlow R, Varki NM, and Chang CL (2004). A fluorescent orthotopic mouse model for reliable measurement and genetic modulation of human neuroblastoma metastasis. *Clin Exp Metastasis* **21**, 563–570.

[16] Ziegler MM, Ishizu H, Nagabuchi E, Takada N, and Arya G (1997). A comparative review of the immunobiology of murine neuroblastoma and human neuroblastoma. *Cancer* **79**, 1757–1766.

[17] Bogenmann E (1996). A metastatic neuroblastoma model in SCID mice. *Int J Cancer* **67**, 379–385.

[18] Morikawa K, Walker SM, Jessup JM, and Fidler IJ (1988). *In vivo* selection of highly metastatic cells from surgical specimens of different primary human colon carcinomas implanted into nude mice. *Cancer Res* **48**, 1943–1948.

[19] Onn A, Isobe T, Itasaka S, Wu W, O'Reilly MS, Ki Hong W, Fidler IJ, and Herbst RS (2003). Development of an orthotopic model to study the biology and therapy of primary human lung cancer in nude mice. *Clin Cancer Res* **9**, 5532–5539.

[20] Bruns CJ, Harbison MT, Kuniyasu H, Eue I, and Fidler IJ (1999). *In vivo* selection and characterization of metastatic variants from human pancreatic adenocarcinoma by using orthotopic implantation in nude mice. *Neoplasia* **1**, 50–62.

[21] Matsui T, Ota T, Ueda Y, Tanino M, and Odashima S (1998). Isolation of a highly metastatic cell line to lymph node in human oral squamous cell carcinoma by orthotopic implantation in nude mice. *Oral Oncol* **34**, 253–256.

[22] Li Y, Tian B, Yang J, Zhao L, Wu X, Ye SL, Liu YK, and Tang ZY (2004). Stepwise metastatic human hepatocellular carcinoma cell model system with multiple metastatic potentials established through consecutive *in vivo* selection and studies on metastatic characteristics. *J Cancer Res Clin Oncol* **130**, 460–468.

[23] Biedler JL, Roffler-Tarlov S, Schachner M, and Freedman LS (1978). Multiple neurotransmitter synthesis by human neuroblastoma cell lines and clones. *Cancer Res* **38**, 3751–3757.

[24] Pietsch T, Gottert E, Meese E, Blin N, Feickert HJ, Riehm H, and Kovacs G (1988). Characterization of a continuous cell line (MHH-NB-11) derived from advanced neuroblastoma. *Anticancer Res* **8**, 1329–1333.

[25] Parham P, Barnstable CJ, and Bodmer WF (1979). Use of a monoclonal antibody (W6/32) in structural studies of HLA-A,B,C, antigens. *J Immunol* **123**, 342–349.

[26] Ozato K and Sachs DH (1981). Monoclonal antibodies to mouse MHC antigens: III. Hybridoma antibodies reacting to antigens of the H-2b haplotype reveal genetic control of isotype expression. *J Immunol* **126**, 317–321.

[27] Halachmi E and Witz IP (1989). Differential tumorigenicity of 3T3 cells transformed *in vitro* with polyoma virus and *in vivo* selection for high tumorigenicity. *Cancer Res* **49**, 2383–2389.

[28] Warzynski MJ, Graham DM, Axtell RA, Higgins JV, and Hammers YA (2002). Flow cytometric immunophenotyping test for staging/monitoring neuroblastoma patients. *Cytometry* **50**, 298–304.

[29] Goldberg-Bittman L, Sagi-Assif O, Meshel T, Nevo I, Levy-Nissenbaum O, Yron I, Witz IP, and Ben-Baruch A (2005). Cellular characteristics of neuroblastoma cells: regulation by the ELR-CXC chemokine CXCL10 and expression of a CXCR3-like receptor. *Cytokine* **29**, 105–117.

[30] Fulda S, Honer M, Menke-Moellers I, and Berthold F (1995). Antiproliferative potential of cytostatic drugs on neuroblastoma cells *in vitro*. *Eur J Cancer* **31A**, 616–621.

[31] Blatt J and Stitely S (1987). Antineuroblastoma activity of desferoxamine in human cell lines. *Cancer Res* **47**, 1749–1750.

[32] Becton DL and Bryles P (1988). Deferoxamine inhibition of human neuroblastoma viability and proliferation. *Cancer Res* **48**, 7189–7192.

[33] Donfrancesco A, Deb G, Dominici C, De Sio L, Inserra A, Boglino C, Takahashi M, Uchino J, and Helson L (1995). D-CECaT as preoperative chemotherapy for unresectable neuroblastoma in children over one year of age. *Anticancer Res* **15**, 2347–2350.

[34] Donfrancesco A, De Bernardi B, Carli M, Mancini A, Nigro M, De Sio L, Casale F, Bagnulo S, Helson L, and Deb G (1995). Deferoxamine followed by cyclophosphamide, etoposide, carboplatin, thiotepa, induction regimen in advanced neuroblastoma: preliminary results. Italian Neuroblastoma Cooperative Group. *Eur J Cancer* **31A**, 612–615.

[35] Deryugina EI and Quigley JP (2006). Matrix metalloproteinases and tumor metastasis. *Cancer Metastasis Rev* **25**, 9–34.

[36] Overall CM and Kleifeld O (2006). Tumour microenvironment—opinion: validating matrix metalloproteinases as drug targets and anti-targets for cancer therapy. *Nat Rev Cancer* **6**, 227–239.

[37] Brahimi-Horn C and Pouyssegur J (2006). The role of the hypoxia-inducible factor in tumor metabolism growth and invasion. *Bull Cancer* **93**, E73–E80.

[38] Subarsky P and Hill RP (2003). The hypoxic tumour microenvironment and metastatic progression. *Clin Exp Metastasis* **20**, 237–250.

[39] Hirota K and Semenza GL (2006). Regulation of angiogenesis by hypoxia-inducible factor 1. *Crit Rev Oncol Hematol* **59**, 15–26.

[40] Minn AJ, Gupta GP, Siegel PM, Bos PD, Shu W, Giri DD, Viale A, Olshen AB, Gerald WL, and Massague J (2005). Genes that mediate breast cancer metastasis to lung. *Nature* **436**, 518–524.

[41] Cheung NV and Cohn SL (2005). *Neuroblastoma.* Heidelberg, Germany: Springer.

[42] Ross RA, Spengler BA, Domenech C, Porubcin M, Rettig WJ, and Biedler JL (1995). Human neuroblastoma I-type cells are malignant neural crest stem cells. *Cell Growth Differ* **6**, 449–456.

[43] Rettig WJ, Spengler BA, Chesa PG, Old LJ, and Biedler JL (1987). Coordinate changes in neuronal phenotype and surface antigen expression in human neuroblastoma cell variants. *Cancer Res* **47**, 1383–1389.

[44] Keshelava N, Seeger RC, Groshen S, and Reynolds CP (1998). Drug resistance patterns of human neuroblastoma cell lines derived from patients at different phases of therapy. *Cancer Res* **58**, 5396–5405.

[45] Biedler JL, Helson L, and Spengler BA (1973). Morphology and growth, tumorigenicity, and cytogenetics of human neuroblastoma cells in continuous culture. *Cancer Res* **33**, 2643–2652.

[46] Tsuruo T and Fidler IJ (1981). Differences in drug sensitivity among tumor cells from parental tumors, selected variants, and spontaneous metastases. *Cancer Res* **41**, 3058–3064.

[47] Spengler BA, Ross RA, and Biedler JL (1986). Differential drug sensitivity of human neuroblastoma cells. *Cancer Treat Rep* **70**, 959–965.

[48] Bjorklund M and Koivunen E (2005). Gelatinase-mediated migration and invasion of cancer cells. *Biochim Biophys Acta* **1755**, 37–69.

[49] Ribatti D, Surico G, Vacca A, De Leonardis F, Lastilla G, Montaldo PG, Rigillo N, and Ponzoni M (2001). Angiogenesis extent and expression of matrix metalloproteinase-2 and -9 correlate with progression in human neuroblastoma. *Life Sci* **68**, 1161–1168.

[50] Sugiura Y, Shimada H, Seeger RC, Laug WE, and DeClerck YA (1998). Matrix metalloproteinases-2 and -9 are expressed in human neuroblastoma: contribution of stromal cells to their production and correlation with metastasis. *Cancer Res* **58**, 2209–2216.

[51] Mohamed MM and Sloane BF (2006). Cysteine cathepsins: multifunctional enzymes in cancer. *Nat Rev Cancer* **6**, 764–775.

[52] Geminder H, Sagi-Assif O, Goldberg L, Meshel T, Rechavi G, Witz IP, and Ben-Baruch A (2001). A possible role for CXCR4 and its ligand, the CXC chemokine stromal cell–derived factor-1, in the development of bone marrow metastases in neuroblastoma. *J Immunol* **167**, 4747–4757.

[53] Nevo I, Sagi-Assif O, Meshel T, Geminder H, Goldberg-Bittman L, Ben-Menachem S, Shalmon B, Goldberg I, Ben-Baruch A, and Witz IP (2004). The tumor microenvironment: CXCR4 is associated with distinct protein expression patterns in neuroblastoma cells. *Immunol Lett* **92**, 163–169.

[54] Holland JD, Kochetkova M, Akekawatchai C, Dottore M, Lopez A, and McColl SR (2006). Differential functional activation of chemokine receptor CXCR4 is mediated by G proteins in breast cancer cells. *Cancer Res* **66**, 4117–4124.

[55] Palmesino E, Moepps B, Gierschik P, and Thelen M (2006). Differences in CXCR4-mediated signaling in B cells. *Immunobiology* **211**, 377–389.

[56] Wang GL and Semenza GL (1993). Desferrioxamine induces erythropoietin gene expression and hypoxia-inducible factor 1 DNA-binding activity: implications for models of hypoxia signal transduction. *Blood* **82**, 3610–3615.

[57] Elstner A, Holtkamp N, and von Deimling A (2007). Involvement of Hif-1 in desferrioxamine-induced invasion of glioblastoma cells. *Clin Exp Metastasis* **24**, 57–66.

[58] Sullivan R and Graham CH (2007). Hypoxia-driven selection of the metastatic phenotype. *Cancer Metastasis Rev* **26**, 319–331.

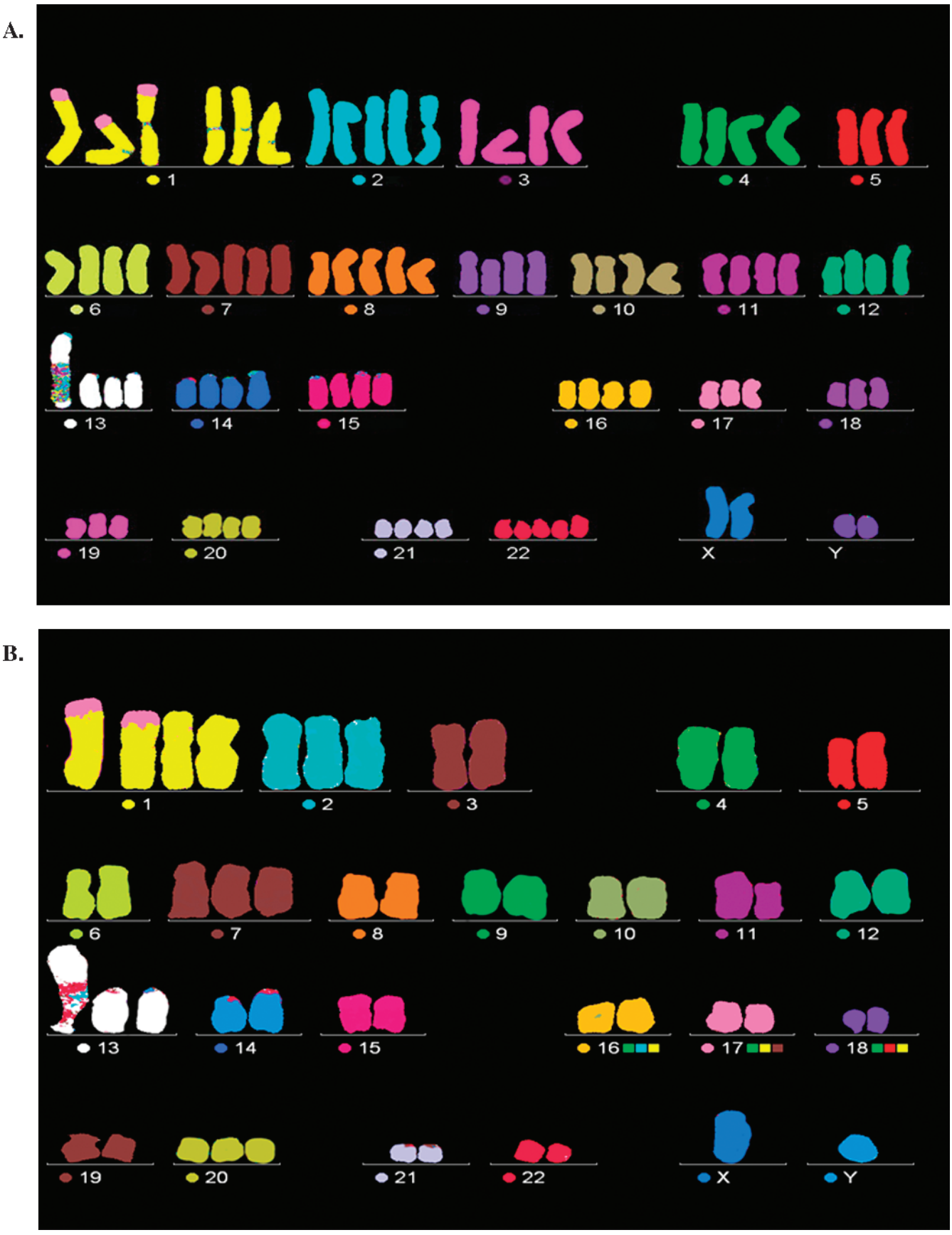

Figure W1. Representative karyotypes of the parental cell line MHH-NB-11 (A), the local variant MHH.Ad (B), and the metastatic variant MHH.Lu3 (C).

C.

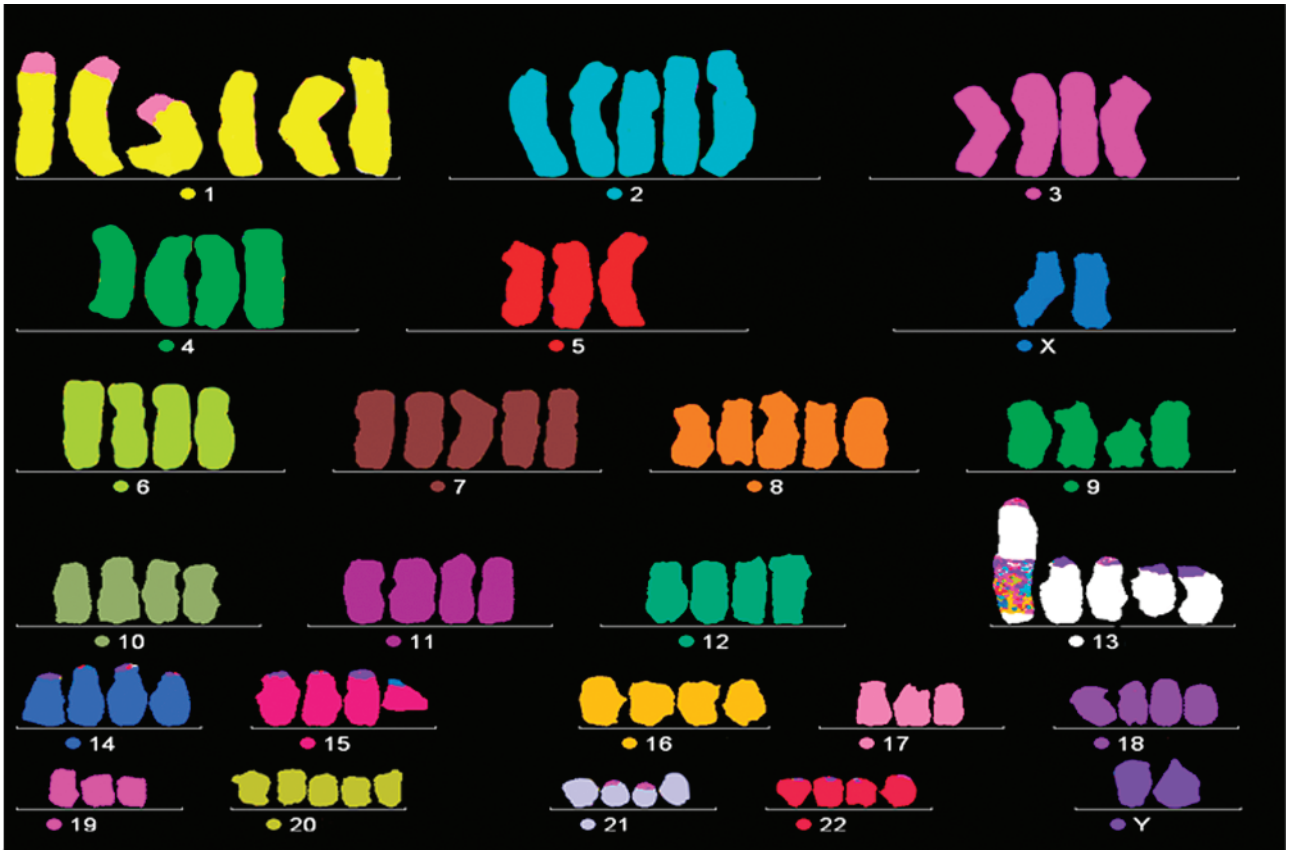

Figure W1. (*continued*)